



OPEN

Magnetic Dipole Impact on the Hybrid Nanofluid Flow over an Extending Surface

Taza Gul^{1,2}, Abbas Khan¹, Muhammad Bilal¹, Nasser Aedh Alreshidi³, Safyan Mukhtar⁴, Zahir Shah⁵ & Poom Kumam^{6,7}✉

The main features of present numerical model is to explore and compare the behavior of simple and hybrid nanoparticles, which were allowed to move on a spreading sheet. The effect of magnetic dipole on hybrid nanofluid flow is considered. A magnetic dipole combined with hybrid nanofluid plays a vital role in controlling the momentum and thermal boundary layers. In view of the impacts of a magnetic dipole on the simple and hybrid nanofluids, steady, laminar and boundary layer flow of Cu/H_2O and $Cu - Al_2O_3/H_2O$ are characterized in this analysis. The governing equations of flow problem are diminished to ordinary differential equation (ODE's) by using similarity approach. For the numerical solution of the nonlinear ODE's, Runge Kutta order 4th technique has been executed. The impact of various physical constraints, such as volume friction, viscous dissipation, Prandtl number and so on have been sketched and briefly discussed for velocity and temperature profile. In this work, some vital characteristics such as skin friction, Curie temperature and local Nusselt number are chosen for physical and numerical analysis. It has been noted that the hybrid nanofluid is more efficient in thermal conduction due to its strong thermal characteristics as compared to simple nanofluid. From results, it is also observed that the turbulence of fluid flow can be controlled through magnetic dipole.

From few last decades, the study over a spreading sheet of conducting fluid and boundary layer flow has received the attention of scientist, researchers and engineers. The MHD (magneto hydrodynamics) subject vast applicability to geophysics, solar physics and energy research. They have several applications in industrial and engineering processes, such as aerodynamics field, electrostatic filters and heat changes, MHD accelerators, extrusion of plastic and metals, paper production and glass fiber, rolling hot wire and crystal growing. The exact solution of steady incompressible viscous fluid flow over a stretching sheet was investigated by Crane¹. Oauf² studied the MHD flow under the thermal radiation effect over a porous stretching sheet and find its exact solution. The mass transfer and MHD flow with chemically reactive species, over linearly stretching sheet was discussed by Takhar *et al.*³. The convective heat transfer and nanofluid flow with the Lorentz force was investigated by Sheikholeslami⁴. An extension was made, by using two phase model to thermal radiation on the nanofluid by Sheikholeslami⁵.

The rapid advancement in almost every field of science and technology has compelled the researchers and scientists to develop the new ideas and imply these in the modern equipment and devices used in the mechanical, electrical and industries, such as heat exchangers, electronic cooling, car radiators, solar thermal, energy storage and heat pipes⁶⁻⁸. In the early age simple liquids like water, oil etc., were applied for heat conduction and transfer of heat, which have very poor thermal conductivity. Later on, in 1995, with the advancement of nanotechnology a new fluid called nanofluid was introduced by Chinese researcher Choi *et al.*⁹. They verified experimentally, that nanofluids comparatively shows more thermal conductivity and efficiency for heat transfer rate than simple or

¹Department of mathematics, City University of Science and Information Technology, Peshawar, Pakistan. ²Higher Education Department Khyber Pakhtunkhwa, Peshawar, Pakistan. ³Department of Mathematics College of Science Northern Border University, Arar, 73222, Saudi Arabia. ⁴Department of Basicnces, Deanship of Preparatory Year, King Faisal University, Hofuf, 31982, Al Ahsa, Saudi Arabia. ⁵Center of Excellence in Theoretical and Computational Science (TaCS-CoE), SCL 802 Fixed Point Laboratory, Science Laboratory Building, King Mongkut's University of Technology Thonburi (KMUTT), 126 Pracha-Uthit Road, Bang Mod, Thung Khru, Bangkok, 10140, Thailand. ⁶KMUTT Fixed Point Research Laboratory, Room SCL 802 Fixed Point Laboratory, Science Laboratory Building, Department of Mathematics, Faculty of Science, King Mongkut's University of Technology Thonburi (KMUTT), 126 Pracha-Uthit Road, Bang Mod, Thung Khru, Bangkok, 10140, Thailand. ⁷Department of Medical Research, China Medical University Hospital, China Medical University, Taichung, 40402, Taiwan. ✉e-mail: poom.kum@kmutt.ac.th

base fluids used in different equipment. The applications of nanofluid in different devices have shown great potential for heat transfer. The influence of particle migration on thermo physical characteristics of nanoparticles studied by Mehdi¹⁰. Hashemi *et al.*¹¹ scrutinized natural convection inside incinerator-shaped cavity loaded with $Al_2O_3 - H_2O$. Seyyed *et al.*¹² investigated magnetized $Al_2O_3 - H_2O$ nano-size particles on entropy optimization in L-shaped cavity. The heat transfer behavior of $Fe_3O_4 - H_2O$ nanofluid inside a semi-circular cavity is analyzed by Dogonchi *et al.*¹³. Zahra *et al.*¹⁴ explored the role of nanoparticles and wavy circular heater on heat transfer inside circular heater. Heris *et al.*¹⁵ experimentally investigated the convective heat transfer flow of oxide. Heris *et al.*¹⁶ experimentally examine the convective heat transfer of Cu - water, CuO - water and Al_2O_3 - water nanofluids and reported the study under laminar condition, the influence of Peclet number, particle volume fraction and nanoparticle source on heat transfer have been examined.

In the new era of emerging technology, a modified class of nanofluids has been developed and named them, the hybrid nanofluids. The hybrid nanofluids are composed of more than one metallic nanoparticle unlike nanofluids which composed of single metal nanoparticles. As, for example Aluminum Oxide nanoparticles are dispersed in water to get a simple nanofluid, but when Copper metallic nanoparticles are added to the same suspension of Alumina/water another kind of nanofluid is obtained called hybrid nanofluid. In the modern age, hybrid nanofluids due their high efficiency in the heat transfer rate and hence high thermal conductivity have attracted a lot of researchers and scientists to this new field of nanotechnology. The importance of hybrid nanofluid in the heat enhancement rate has been studied in the relevant literature by Nadeem *et al.*¹⁷ explored the characteristic of hybrid nanofluid in three-dimensional stagnation point flow and obtained the rate, thermal transforming in hybrid nanofluids are comparatively more than simple nanofluid. Suresh *et al.*¹⁸ examine the properties of the Hybrid nanofluid movement and transfer of heat phenomena. Gorla *et al.*¹⁹ explore natural convection as well as the transfer of heat flow using source/sink effect on $Cu - Al_2O_3/H_2O$ hybrid nanofluid. They obtained hybrid suspension by making changes in the position of heat sources and Nusselt number diminished appreciably. Tayebi *et al.*²⁰ use two confocal elliptical cylinders, one containing $Cu - Al_2O_3$ / water hybrid nanofluid and the other containing simple nanofluid Al_2O_3 / water and examined natural convection in an annulus and found that the more heat is transferred through $Cu - Al_2O_3$ / water than to the simple nanofluid Al_2O_3 / water. Tayebi *et al.*²¹ used an eccentric horizontal cylindrical annulus to investigate the natural convection of hybrid nanofluid. Chamkha *et al.*²² examined the transfer of heat and magnetohydrodynamic flow of hybrid nanofluid using rotating system. Magnetic field effect on stagnation flow of a $TiO_2 - Cu$ / water hybrid nanofluid has been analyzed over an extending sheet²³. experimentally investigated the heat transfer characteristics of Graphene Oxide / CO_3O_4 hybrid nanofluids. Wei *et al.*²⁴ evaluated the thermo physical properties of diathermic oil based hybrid nanofluids for heat transfer applications. Yarmand *et al.*²⁵ examined the enhanced heat transfer rate for graphene nanoplatelets-silver hybrid nanofluids. Yarmand *et al.*²⁶ conducted the study of the synthesis, stability and thermal-physical properties of graphene nanoplatelets/platinum hybrid nanofluids. Yarmand *et al.*²⁷ analyzed the enhancement of heat transfer rate using the graphene nano platelets/platinum hybrid nanofluids. Abbasi *et al.*²⁸ used hybrids of carbon nanotubes/gamma alumina to analyze the stability and thermal conductivity of the nanofluid using functionalization method. Sajid *et al.*²⁹ conducted numerically and experimentally intensive studies on thermophysical properties of hybrid as well as single form nanotubes. They concluded and suggested that the thermophysical properties of nanofluid are greatly affected by nanoparticles size, types, concentration and temperature and PH variation.

The proper selection of nanoparticles for base fluid plays a vital role in achieving hybrid nanofluid stability. Van Trinh *et al.*³⁰ experimentally studied hybrid nanofluid by adding Gr (Graphene) carbon nanotubes in ethylene glycol based fluid using ultrasonic techniques. They measured thermal conductivity of Graphene CNTs nanofluid by using GHP (guarded hotplate) technique. The transformer is mostly used in distribution and transmission system. For its cooling and insulation vegetable oil and mineral oil were used for last few decades. But almost 75% of the total failed, due to improper electric insulation and high voltage power of transformer. By using Taguchi methodology, Sumathi³¹ *et al.* investigated the transformer dielectric strength of $TiO_2/MoS_2/Al_2O_3$ hybrid nanofluid. Gupta *et al.*³² made a comprehensive review on the study related to the demand and interest of nanofluids with the transfer of heat. Furthermore, in their research articles, they briefly discussed the preparation and thermal characteristics of hybrid nanofluid. Valan and Dhinesh Kumar³³ examined the properties, stability, characteristics and synthesis of hybrid nanofluid. Valnes and Anderson³⁴ considered ferrofluid flow under the effects of magnetic dipole over a stretching sheet.

The study of hybrid nanofluid is quite important in several fields of science and engineering. The purpose of the present work is to examine the influence of magnetic dipole on the hybrid nanofluid flow over extending surface, which is based with no slip condition and non porous medium. The concern work is the extension of³⁴. To investigate the $Cu - Al_2O_3/H_2O$ hybrid nanofluid flow and improve its thermophysical properties under magnetic dipole is the main objective of the paper. The present work has many applications; such as the hybrid nanofluids is mostly used in ultra-capacitors, atomic reactors, textile engineering, nonporous cleaner, gas storing, different kinds of coating and in the bio sensors, which make this work more valuable. The system of ODEs diminishes from the system of PDEs through similarity approach. The numerical solution of the problem is drawn via Runge Kutta order four method.

Mathematical formulation of the problem

In this study, we consider two types of nanofluids, one is simple nanofluid comprising one nanoparticle of metal Copper dispersed in base fluid water (Cu/H_2O) and the other is the modified nanofluid (hybrid nanofluid) consist of nanoparticles of Copper and aluminum oxide mixed in water ($Cu - Al_2O_3/H_2O$). For two sorts of fluids, the flow and thermal equations are given as below;

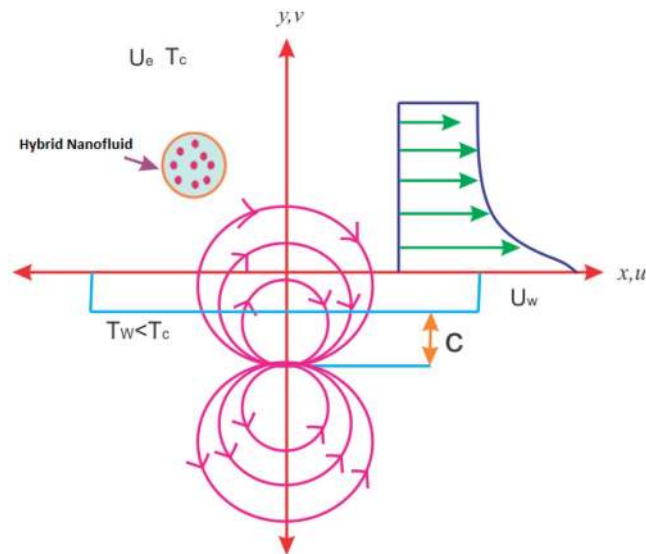


Figure 1. Geometry of the problem.

Hydrodynamic and thermal energy equations

Flow analysis. For flow analysis, we consider two nanofluid flows Cu/H_2O and $Cu - Al_2O_3/H_2O$, which are laminar, steady and having incompressible viscous boundary layers taken over an extending sheet as shown in the schematic diagram. The fluid flow is from left to right in the direction of positive x-axes. For constant magnetic field, the magnetic dipoles are taken exactly along y-axes at a distance can depicts form figure. Since the sheet is flexible, this can cause flow due to extending. Suppose the velocity of the extending sheet or wall is $U_w = Sx$ (S is a dimensionless constant) and T_w specifies the temperature of the stretching wall, while T_c denotes the Curie temperature above the surface of the fluid and cannot be magnetized. Also, it is suppose that $T = T_\infty$ is the temperature of the fluid such that $T_w < T_\infty < T_c$. The cited boundary layer approximation Andersson *et al.*³⁴, Zeeshan *et al.*³⁵ and Muhammad *et al.*³⁶ is taken into account as $O(u) = O(x) = O(1)$ and $O(v) = O(y) = O(\infty)$. The round lines with arrows in the figure show the magnetic field effect. The schematic diagram for the flow analysis is depicted from Fig. 1. Ferrohydrodynamic boundary layers flow equations in two dimensions of mass conservation, fluid momentum and thermal energy are given below;

$$\frac{\partial u}{\partial x} + \frac{\partial v}{\partial y} = 0 \quad (1)$$

$$\rho_{hnf} \left(u \frac{\partial u}{\partial x} + v \frac{\partial u}{\partial y} \right) = - \frac{\partial P}{\partial x} + \mu_f M \frac{\partial H}{\partial x} + \mu_{hnf} \frac{\partial^2 u}{\partial y^2}, \quad (2)$$

$$(\rho C_p)_{hnf} \left(u \frac{\partial T}{\partial x} + v \frac{\partial T}{\partial y} \right) = K_{hnf} \frac{\partial^2 T}{\partial y^2} - \left(u \frac{\partial H}{\partial x} + v \frac{\partial H}{\partial y} \right) \mu_f T \frac{\partial M}{\partial x}. \quad (3)$$

The above three main equations are taken for fluid flow in the presence of viscous dissipation. Since the flow is in two dimensions, therefore velocity has two components, (u) is along x-axes and (v) is along y-axes. In the above second equation ρ_{hnf} , μ_{hnf} , μ_f and M represent the density of the nanofluid, dynamic viscosity of the nanofluid, permeable magnetic field and magnetization of the magnetic field respectively. In the third equation $(\rho C_p)_{hnf}$ depicts specific heat of the nanofluid and K_{hnf} is used for thermal conductivity of the hybrid nanofluid, whereas T and H are used for temperature and magnetic field respectively. Let the appropriate boundary conditions used by refs. ^{34,35} are taken for the boundary value problem.

$$u|_{y=0} = U_w = Sx, v|_{y=0} = 0, T|_{y=0} = T_w, u|_{y \rightarrow \infty} \rightarrow 0, T|_{y \rightarrow \infty} \rightarrow T_\infty = T_c. \quad (4)$$

Temperature at different points is taken with appropriate boundary conditions at $y = 0$ and $y \rightarrow \infty$, as defined earlier, the Curie temperature (T_c) and the ambient temperature (T_∞).

Magnetic dipole. When a magnetic field is applied, the flow of nanofluid will be affected over spreading sheet and cause a magnetic field region represented by δ_1 and mathematically expressed as ref. ³⁵;

$$\delta_1 = \frac{\gamma_1 x}{2\pi x^2 + (y + c)^2}. \quad (5)$$

In the above equation, strong point of the magnetic field at the base is indicated by γ_1 , while c specifies the displacement of magnetic dipole. Components of magnetic field (H) are taken mathematically as;

$$H_x = -\frac{\partial \delta_1}{\partial x} = \frac{\gamma_1}{2\pi} \frac{x^2 - (y + c)^2}{(x^2 + (y + c)^2)^2}, \quad (6)$$

$$H_y = -\frac{\partial \delta_1}{\partial y} = \frac{\gamma_1}{2\pi} \frac{2x(y + c)}{(x^2 + (y + c)^2)^2}. \quad (7)$$

Differentiating Eq. (5) with respect to x and y , we get the above two expressions for magnetic field components. Magnetic force has direct relation with a gradient of H therefore norm of H can mathematically be expressed as;

$$H = \sqrt{\left(\frac{\partial \delta_1}{\partial x}\right)^2 + \left(\frac{\partial \delta_1}{\partial y}\right)^2}. \quad (8)$$

By inserting the values in the above equation, we obtained the following equations.

$$\frac{\partial H}{\partial x} = \frac{\gamma_1}{2\pi} \frac{2x}{(y + c)^4}, \quad (9)$$

$$\frac{\partial H}{\partial x} = \frac{\gamma_1}{2\pi} \left[-\frac{2}{(y + c)^3} + \frac{4x^2}{(y + c)^5} \right]. \quad (10)$$

Since variation in temperature can cause change in magnetization therefore impacts on magnetization can mathematically be expressed as

$$M = K_1(T - T_\infty). \quad (11)$$

Here M is used for magnetization while pyro-magnetic coefficient is indicated by K_1 in the above expression.

Transformation. In order to transform the main equation, we use the dimensionless variables as introduced by ref. ³⁶.

$$\psi(\eta, \xi) = \left(\frac{\mu_f}{\rho_f}\right) \eta f(\xi), \quad \theta(\eta, \xi) = \frac{T_c - T}{T_c - T_w} = \theta_1(\xi) + \eta^2 \theta_2(\xi), \quad (12)$$

Here, $\theta_1(\eta, \xi)$ and $\theta_2(\eta, \xi)$ indicate the non-dimensional temperature terms and μ_f specifies fluid viscosity. The non-dimensional and consistent coordinates can be expressed as;

$$\xi = y \left(\frac{\rho_f S}{\mu_f}\right)^{\frac{1}{2}}, \quad \eta = x \left(\frac{\rho_f S}{\mu_f}\right)^{\frac{1}{2}}. \quad (13)$$

Continuity equations are satisfied directly by the function described and the velocity components achieved as;

$$u = \frac{\partial \psi}{\partial y} = S x f'(\xi), \quad v = \frac{\partial \psi}{\partial x} = -\left(S \mu_f\right)^{\frac{1}{2}} f(\xi). \quad (14)$$

$f'(\xi)$ denotes first derivative with respect to ξ .

Thermo-physical properties. The active density ρ_{hnf} and heat capacitance $(\rho C_p)_{hnf}$ of the simple nanofluid Cu / water and the hybrid nanofluid ($Cu - Al_2O_3$) as used by ref. ²¹ are as follows:

$$\frac{\rho_{hnf}}{\rho_f} = \left[(1 - \phi_2) \left\{ (1 - \phi_1) + \phi_1 \frac{\rho_{s1}}{\rho_f} \right\} + \phi_2 \frac{\rho_{s2}}{\rho_f} \right], \quad (15)$$

$$\frac{(\rho C_p)_{hnf}}{(\rho C_p)_f} = \left[(1 - \phi_2) \left\{ (1 - \phi_1) + \phi_1 \frac{(\rho C_p)_{s1}}{(\rho C_p)_f} \right\} + \phi_2 \frac{(\rho C_p)_{s2}}{(\rho C_p)_f} \right]. \quad (16)$$

ϕ_1 and ϕ_2 are used for the solid volume fraction of Al_2O_3 and Cu respectively in the above modeled equations. ρ_{s1} and ρ_{s2} specify the density for both nanofluids while ρ_f is used for density of base fluid. Heat capacitance is indicated by $(\rho C_p)_{s1}$ and $(\rho C_p)_{s2}$ respectively for both nanofluids, where as $(\rho C_p)_f$ is used for heat capacitance of base fluid.

Simple nanofluid as well as the hybrid nanofluid, satisfies the dynamic viscosities which discussed by Rashidi *et al.*³⁷ and Hayat *et al.*³⁸ and is deliberated as;

$$A_1 = \frac{\mu_{hnf}}{\mu_f} = (1 - \phi_1)^{-2.5} (1 - \phi_2)^{-2.5}. \quad (17)$$

Thermal conductivity for both the nanoparticles dispersed in water studied at Lee *et al.*³⁹, and Wang *et al.*⁴⁰

$$A_2 = \frac{K_{hnf}}{K_f} = \left(\frac{K_{s2} + (n-1)K_{bf} - (n-1)\phi_2(K_{bf} - K_{s2})}{K_{s2} + (n-1)K_{bf} + \phi_2(K_{bf} - K_{s2})} \right). \quad (18)$$

where

$$\frac{K_{bf}}{K_f} = \frac{K_{s1} + (n-1)K_f - (n-1)\phi_1(K_f - K_{s1})}{K_{s1} + (n-1)K_f + \phi_1(K_f - K_{s1})}. \quad (19)$$

Plugging the above mentioned thermo-physical properties and transformation; both the momentum and thermal boundary layers became as below;

$$\frac{1}{A_1 \rho_{hnf}} f''' - f'^2 + ff'' - \frac{2\beta\theta_1}{\rho_{hnf}} (\xi + \gamma^*)^4 = 0, \quad (20)$$

$$\frac{A_2}{(\rho C_p)_{hnf}} \theta''_1 + Pr_f \left(f\theta'_1 - 2f'\theta_1 \right) + \frac{2\beta\lambda f(\theta_1 - \varepsilon)}{(\varepsilon + \gamma^*)^3} - 4\lambda f'^2 = 0, \quad (21)$$

$$\frac{A_2}{(\rho C_p)_{f\theta'_1 - 2f'\theta_1}} \theta''_2 - Pr_f \left(4f\theta'_2 - f'\theta_2 \right) + \frac{2\beta\lambda f\theta_2}{(\varepsilon + \gamma^*)^3} - \lambda\beta(\theta_1 - \varepsilon) \left(\frac{2f'}{(\varepsilon + \gamma^*)^4} + \frac{4f}{(\varepsilon + \gamma^*)^5} \right) - \lambda f'^2 = 0. \quad (22)$$

$$\begin{aligned} f(0) = 0, f'(0) = 1, f'(\infty) = 0, \\ \theta_1(0) = 1, \theta_1(\infty) = 0, \theta_2(0) = 0, \theta_2(\infty) = 0. \end{aligned} \quad (23)$$

For hydrodynamic interaction the symbol β is used by refs.^{35,36} and is defined by

$$\beta = \frac{\gamma \mu_0 K (T_c - T_w) \rho}{2\pi \mu^2}. \quad (24)$$

Prandtl number Pr. Expressed as

$$Pr = \frac{\nu}{\alpha}. \quad (25)$$

Curie temperature is given by

$$\varepsilon = \frac{T_\infty}{T_c - T_w}. \quad (26)$$

The expression for viscous dissipation is as

$$\lambda = \frac{S\mu^2}{\rho K (T_c - T_w)}. \quad (27)$$

and

$$\gamma^* = \sqrt{\frac{S\rho c^2}{\mu}}. \quad (28)$$

Equation (29) indicates the expression for magnetic field strength. The following formula is used for skin friction coefficient;

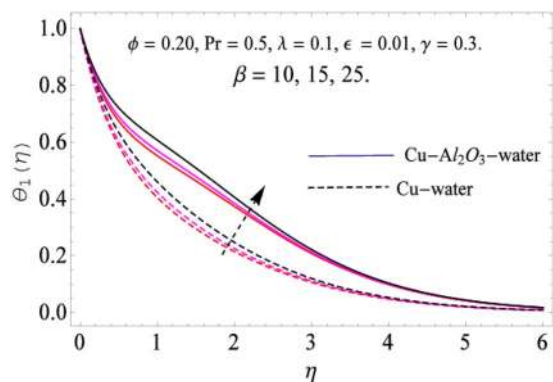


Figure 2. The impact of β (Ferohydrodynamic) versus Temperature-1.

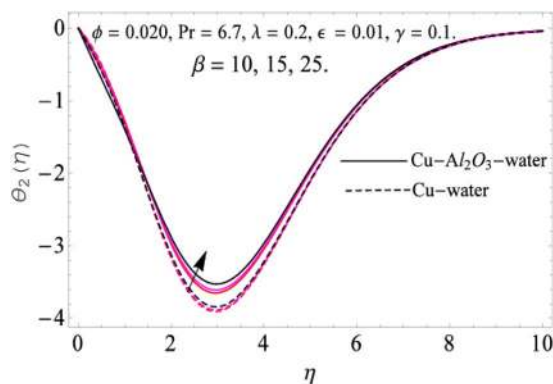


Figure 3. The impact of β (Ferohydrodynamic) versus Temperature-2.

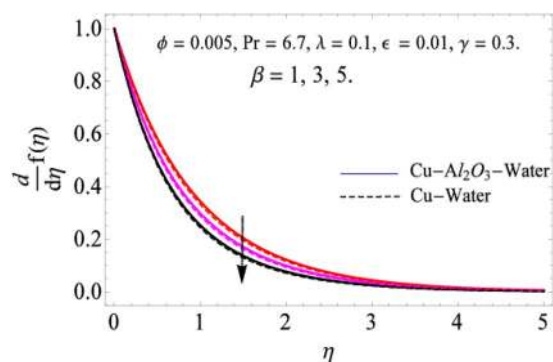


Figure 4. The impact of β (Ferohydrodynamic) versus Velocity.

$$C_f = \frac{-2\tau_w}{\rho_{hmf} U_w^2} \tag{29}$$

where

$$\tau_w = \mu_{hmf} \left. \frac{\partial u}{\partial y} \right|_{y=0} \tag{30}$$

Whereas the Nusselt number can be written mathematically as;

$$Nu = \frac{x K_{hmf}}{K_f (T_c - T_w)} \left. \frac{\partial T}{\partial y} \right|_{y=0} \tag{31}$$

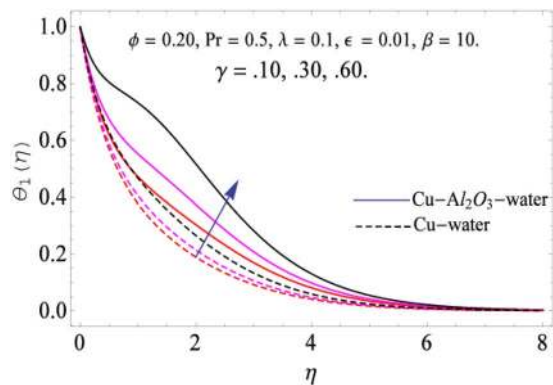


Figure 5. The impact of γ (Magnetic field strength) versus Temperature-1.

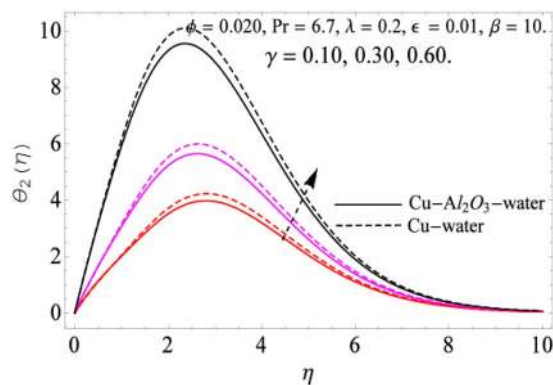


Figure 6. The impact of γ versus Temperature-2.

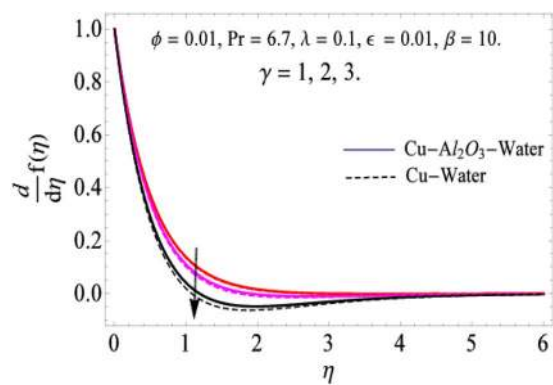


Figure 7. The impact of γ versus Velocity.

Thus, C_f (coefficient of skin friction) and Nu (Nusselt number) with non-dimensional equations as (34,35)

$$\frac{1}{2} \text{Re}_x^{-\frac{1}{2}} C_f = \frac{1}{(1 - \phi_1)^{2.5} (1 - \phi_2)^{2.5}} f'''(0). \tag{32}$$

$$\text{Re}_x^{-\frac{1}{2}} Nu_x = \frac{K_{hmf}}{K_f} (\theta'_1(0) + \eta^2 \theta'_2(0)). \tag{33}$$

Whereas $\text{Re}_x = \frac{xU_w(x)}{V_f \mu} = \frac{Sx^2}{V_f \mu}$, indicates the Reynold's number, depends on the extending rate of change of displacement $U_w(x)$, $\text{Re}_x^{-\frac{1}{2}} C_f$, shows coefficient of skin friction and $\text{Re}_x^{-\frac{1}{2}} Nu_x$ is used for Nusselt number.

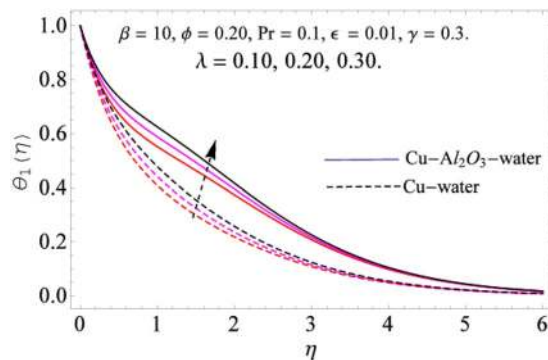


Figure 8. The impact of λ versus Temperature-1.

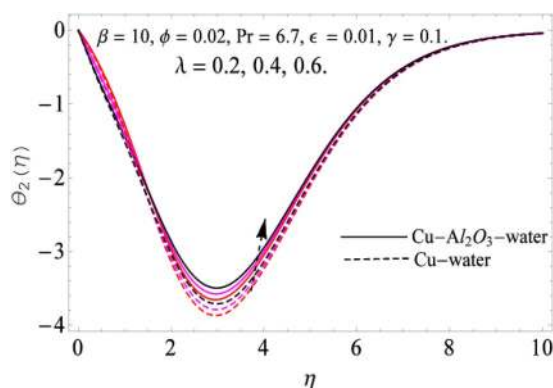


Figure 9. The impact of λ versus Temperature-2.

Solution methodology. In order to use the RK-4 scheme, different values are chosen for transformation, to convert the equations; into first order differential equations. We take the following supposition. $y_1 = f, y_2 = f', y_3 = f'', y_4 = \theta_1, y_5 = \theta_1', y_6 = \theta_2, y_7 = \theta_2'$. Making use of fluid properties and the equation of boundary values, the above three equation of simple nanofluid (Cu/H_2O) and hybrid nanofluid ($Cu - Al_2O_3/H_2O$), be comes as below.

$$\begin{aligned}
 y'_1 = y_2, y'_2 = y_3, y'_3 &= \frac{A_1 \rho_{hmf}}{\rho_f} \left(y_2^2 - y_1 y_3 + \frac{2\beta y_4 \rho_f}{\rho_{hmf} (\xi + \gamma^*)^4} \right), \\
 y'_4 = y_5, y'_5 &= - \frac{(\rho C_p)_{hmf}}{A_2 (\rho C_p)_f} \left(\frac{\text{Pr}_f (y_1 y_5 - 2y_2 y_4) + 2\lambda\beta (y_4 - \varepsilon) (\xi + \gamma^*)^3 - 4\lambda y_2^2}{y_1} \right), \\
 y'_6 = y_7, y'_7 &= - \frac{(\rho C_p)_{hmf}}{A_2 (\rho C_p)_f} \left(\frac{\text{Pr}_f (4y_1 y_9 - 2y_2 y_8) + \frac{2\lambda\beta}{y_1} y_8 (\xi + \gamma^*)^3}{-\lambda\beta (y_4 - \varepsilon) \left(\frac{2y_2}{(\xi + \gamma^*)^4} + \frac{4y_1}{(\xi + \gamma^*)^5} \right)} - \lambda y_3^2 \right), \\
 y_1 = 0, y_2 = 1, y_3 = u_1, y_4 = 1, y_5 = u_2, y_6 = 0, y_7 = u_3.
 \end{aligned} \tag{34}$$

Results and discussions

The governing equations of the problem have been solved numerically using the RK-4 method after using appropriate transformations. Flow analysis and heat transfer effect of simple nanofluid and hybrid nanofluid have been compared graphically. Different parameters like volume fraction, Prandtl number, viscous dissipation, ferrohydrodynamic interaction, magnetic field strength and so on have been analyzed graphically for velocity and temperature distributions of simple and hybrid nanofluids. The effect of ferrohydrodynamic parameter (β) is indicated in Fig. 2, which shows the increment in temperature with the increasing value of ferrohydrodynamic interaction in both the simple and hybrid nanofluid. In fact, when the interaction or collision of molecules of the

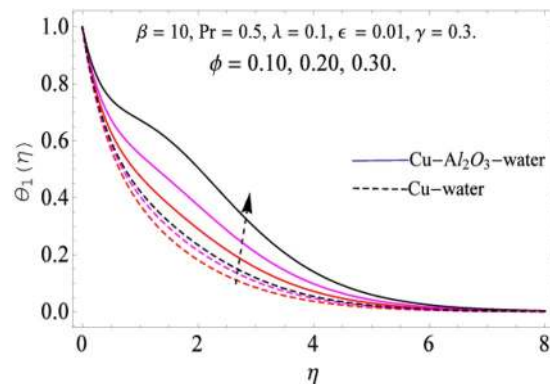


Figure 10. The impact of ϕ versus Temperature-1.

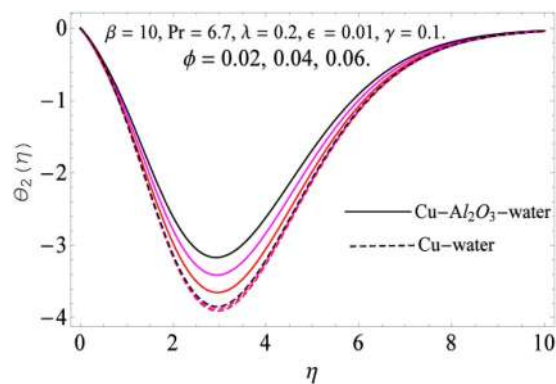


Figure 11. The impact of ϕ versus Temperature-2.

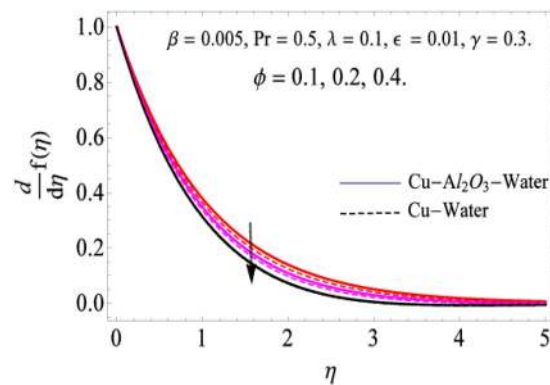


Figure 12. The impact of ϕ versus Velocity.

ferrohydrodynamic metals in the fluids are greater, it will enhance the temperature. The similar effect has been shown at other temperature with slight difference in behavior for both nanofluids as evident from Fig. 3, whereas Fig. 4 specifies the negative effect on velocity profile. This is due to the fact that nanoparticle concentration enhances density of the fluid which consequently reduces the axial velocity of the fluid. Figures 5 and 6 show the impacts of magnetic field strength (γ), which enhances the temperature effect of different terms. The heat transfer effect of hybrid nanofluid is comparatively higher than the simple nanofluid, because of the dispersion nanoparticles of Al_2O_3 in the nanofluid is more influential to magnetic field than the simple nanofluid, as concentration of nanoparticles will increase intermolecular collision and hence increase the kinetic energy which consequently enhances the temperature. Therefore an addition of Al_2O_3 to the $Cu/water$ can cause an increase in heat transfer rate. Wherein, for velocity profile the impacts of the same parameter (γ) have a negative effect as indicated in Fig. 7. The Figs. 8 and 9 demonstrate the effect of viscous dissipation (λ) on temperature distribution. The temperature increases with the increase of viscous dissipation as evident from the figures. As we know that viscosity of a

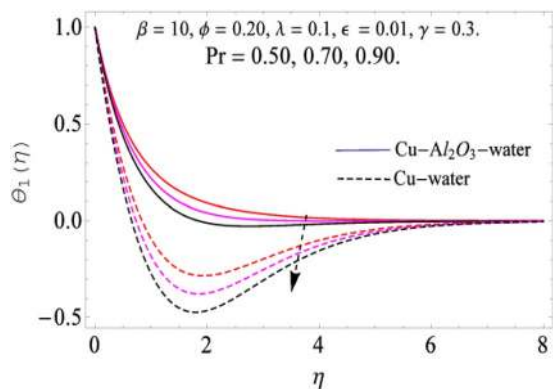


Figure 13. The impact of Pr. versus Temperature-1.

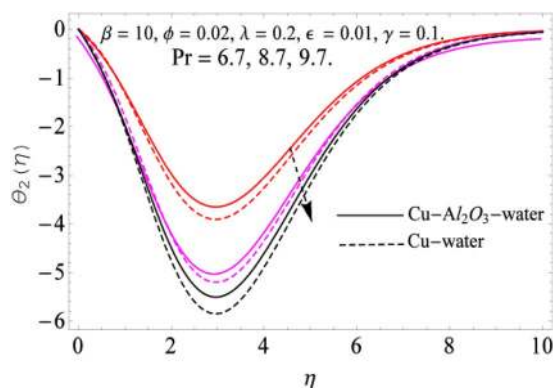


Figure 14. The impact of Pr. versus Temperature-2.

γ	$\sqrt{Re_x} C_f^{36}$	Present	$\frac{Nu_x^{36}}{\sqrt{Re_x}}$	Present
0.1	1.5221	1.5222318	0.5670	0.56713188
0.2	1.5074	1.5075729	0.5765	0.5766750
0.3	1.4884	1.4885273	0.5921	0.5922552
0.4	1.4637	1.4638747	0.6151	0.6152945

Table 1. Comparison with existing literature, excluding dissimilar parameters. When. $Pr = 7, \epsilon = \lambda = 0.3, \beta = c = 1$.

ϕ_1	ϕ_2	β	γ	$Cu - Al_2O_3/H_2O$	Cu/H_2O
0.1	0.1	2	0.3	0.639816	0.63582
0.2				0.998612	
0.3				0.65258	
	0.2				0.989658
	0.3				0.61375
		3		3.11988	2.97985
		4		3.58719	3.54835
			0.4	4.79543	4.27571
			0.5	5.79559	5.25752

Table 2. Skin friction for the Hybrid nanofluid When. $\epsilon = 0.6, Pr = 7.6, c = 1, \lambda = 0.2$.

fluid effect the temperature, so the increasing values of viscous dissipation enhances the hotness of the fluids and hence as a result the temperature boosts up. The impacts of volume fraction over temperature distribution have been mentioned in Figs. 10 and 11. The increment in volume fraction means to increase the nanoparticle in the fluids causes concentration and hence produce hotness which results an increase in temperature field. The velocity distribution has the reverse effect over the increasing values of volume fraction as can be seen from Fig. 12. The

ϕ_1	ϕ_2	Pr	Cu/H ₂ O	Cu – Al ₂ O ₃ /H ₂ O
0.1	0.1	7	1.9234	1.98188
0.2			2.39452	2.49348
0.3			2.88562	2.994988
	0.2		1.96725	1.94758
	0.3		0.948876	0.989986
		7.5	1.99864	2.06123
		7.8	2.1323956	2.345722

Table 3. Nusselt number for the Hybrid nanofluids. When. $\varepsilon = 0.6$, $\gamma = 0.4$, $c = 1$.

impacts of parameter Prandtl Number versus temperature profile have been mentioned in the Figs. 13 and 14, which shows negative effect to the increasing values of Prandtl Number. This is because of the fact that Prandtl Number is a dimensionless number and is the ratio of the hydrodynamic boundary layer to thermal boundary layer or in other words, Pr is the ratio of the molecular diffusivity over thermal diffusivity, therefore the increase of this number will definitely decrease the temperature of the fluids. The comparison of the present study has been compared with the existing literature and shown in Table 1. The variation in the skin friction under the influence of the physical parameters shown in the Table 2. The increasing values of the nanoparticle volume fraction improve the drag force and this effect is relatively stronger using the hybrid nanofluid Cu – Al₂O₃/H₂O. The greater strength of the constraints β & γ , increasing the skin friction. In fact, the magnetic dipole improves the resistive force and boost of the skin friction. Table 3 shows that Nusselt number is the increasing function of the nanoparticle volume fraction and this effect is more prominent in the case of hybrid nanofluid Cu – Al₂O₃/H₂O. The increasing value of the Prandtl number declines the thermal boundary layer and enhancing the Nusselt number as revealed in the Table 3.

Conclusion

In this paper, the study has been conducted to examine and compare the heat transfer effect in simple nanofluid and the hybrid nanofluid flow. All the physical parameters and their effects over temperature and velocity distribution have been shown graphically. These may be summarized as under.

- It has been shown graphically that ferrohydrodynamic parameter (β) and magnetic field strength (γ) have a positive effect over the temperature field, while for velocity distribution it is negative for both nanofluids. It is also noted that hybrid nanofluid shows more efficiency in heat transfer rate than the simple nanofluid in almost for all parameters.
- The impact of viscous dissipation parameter (λ) over the temperature field also shows an increasing trend for both the fluids on different terms of temperature.
- The concentration of volume fraction (ϕ) enhances the temperature field where as the velocity field is reduced due to viscosity because with the addition of nanoparticles the fluid gets dense and hence slow down the movement of the fluid.
- The increase in Prandtl Number has negative impacts over the temperature distribution.
- From the above analysis and graphical representation, we can conclude that the heat transfer effect in the hybrid nanofluid Cu – Al₂O₃/ water is more efficient than the simple nanofluid Cu/ water.
- Keeping in view the significance of the modified nanofluid (hybrid nanofluid), the scientists and researchers may use these for efficient performance in the emerging technologies and for the cooling effects of various electrical and electronic applications.

Received: 10 February 2020; Accepted: 1 April 2020;

Published online: 21 May 2020

References

1. Crane & Lawrence, J. Flow past a stretching plate. *Zeitschrift für angewandte Mathematik und Physik ZAMP* **21**(4), 645–647 (1970).
2. Ouaf & Mahmoud, M. Exact solution of thermal radiation on MHD flow over a stretching porous sheet. *Applied Mathematics and Computation* **170**(2), 1117–1125 (2005).
3. Harmindar, S. *et al.* Flow and mass transfer on a stretching sheet with a magnetic field and chemically reactive species. *International Journal of Engineering Science* **38**(12), 1303–1314 (2000).
4. Sheikholeslami, M. *et al.* Simulation of MHD CuO–water nanofluid flow and convective heat transfer considering Lorentz forces. *Journal of Magnetism and Magnetic Materials* **369**, 69–80 (2014).
5. Sheikholeslami, M., Mohsen, Davood, D., Younus, M. & Ellahi, R. Effect of thermal radiation on magnetohydrodynamics nanofluid flow and heat transfer by means of two phase model. *Journal of Magnetism and Magnetic Materials* **374**, 36–43 (2015).
6. Bahiraei, M. *et al.* Recent research contributions concerning use of nanofluids in heat exchangers: a critical review. *Applied Thermal Engineering* **133**, 137–159 (2018).
7. Bahiraei, M. & Heshmatian, S. Graphene family nanofluids: a critical review and future research directions. *Energy Conversion and Management* **196**, 1222–1256 (2019).
8. Bahiraei, M. & Heshmatian, S. Electronics cooling with nanofluids: a critical review. *Energy Conversion and Management* **172**, 438–456 (2018).
9. Choi, S. U. & Eastman, J. A. Enhancing thermal conductivity of fluids with nanoparticles (No. ANL/MSD/CP-84938; CONF-951135-29). *Argonne National Lab., IL (United States)* (1995).

10. Bahiraei, M. Particle migration in nanofluids: a critical review. *International Journal of Thermal Sciences* **109**, 90–113 (2016).
11. Hashemi, M., Dogonchi, A. S., Seyyedi, S. M., Chamkha, A. J. & Ganji, D. D. Magneto-hydrodynamic natural convection and entropy generation analyses inside a nanofluid-filled incinerator-shaped porous cavity with wavy heater block. *Journal of Thermal Analysis and Calorimetry*, 1–13(2020).
12. Seyyedi, S. M., Dogonchi, A., Hashemi-Tilehnoee, M., Waqas, M. & Ganji, D. D. Entropy generation and economic analyses in a nanofluid filled L-shaped enclosure subjected to an oriented magnetic field. *Applied Thermal Engineering* **168**, 114789 (2020).
13. Dogonchi, A. S., Waqas, M., Seyyedi, S. M., Hashemi-Tilehnoee, M. & Ganji, D. D. A modified Fourier approach for analysis of nanofluid heat generation within a semi-circular enclosure subjected to MFD viscosity. *International Communications in Heat and Mass Transfer* **111**, 104430 (2020).
14. Abdelmalek, Z. *et al.* Role of various configurations of a wavy circular heater on convective heat transfer within an enclosure filled with nanofluid. *International Communications in Heat and Mass Transfer* **113**, 104525 (2020).
15. Heris, S. Z., Etemad, S. G. & Esfahany, M. N. Experimental investigation of oxide nanofluids laminar flow convective heat transfer. *International communications in heat and mass transfer* **33**(4), 529–535 (2006).
16. Heris, S. Z., Esfahany, M. N. & Etemad, S. G. Experimental investigation of convective heat transfer of Al₂O₃/water nanofluid in circular tube. *International journal of heat and fluid flow* **28**(2), 203–210 (2007).
17. Nadeem, S., Abbas, N. & Khan, A. U. Characteristics of three dimensional stagnation point flow of Hybrid nanofluid past a circular cylinder. *Results in physics* **8**, 829–835 (2018).
18. Suresh, S., Venkataraj, K. P., Selvakumar, P. & Chandrasekar, M. Effect of Al₂O₃–Cu/water hybrid nanofluid in heat transfer. *Experimental Thermal and Fluid Science* **38**, 54–60 (2012).
19. Gorla, R., Siddiq, S., Mansour, M. A., Rashad, A. M. & Salah, T. Heat source/sink effects on a hybrid nanofluid-filled porous cavity. *Journal of Thermophysics and Heat Transfer* **31**(4), 847–857 (2017).
20. Tayebi, T. & Chamkha, A. J. Free convection enhancement in an annulus between horizontal confocal elliptical cylinders using hybrid nanofluids. *Numerical Heat Transfer, Part A: Applications* **70**(10), 1141–1156 (2016).
21. Tayebi, T. & Chamkha, A. J. Natural convection enhancement in an eccentric horizontal cylindrical annulus using hybrid nanofluids. *Numerical Heat Transfer, Part A: Applications* **71**(11), 1159–1173 (2017).
22. Chamkha, A. J., Dogonchi, A. S. & Ganji, D. D. Magneto-hydrodynamic flow and heat transfer of a hybrid nanofluid in a rotating system among two surfaces in the presence of thermal radiation and Joule heating. *AIP Advances* **9**(2), 025103 (2019).
23. Sundar, L. S., Singh, M. K., Ferro, M. C. & Sousa, A. C. Experimental investigation of the thermal transport properties of graphene oxide/Co₃O₄ hybrid nanofluids. *International Communications in Heat and Mass Transfer* **84**, 1–10 (2017).
24. Wei, B., Zou, C., Yuan, X. & Li, X. Thermo-physical property evaluation of diathermic oil based hybrid nanofluids for heat transfer applications. *International Journal of Heat and Mass Transfer* **107**, 281–287 (2017).
25. Yarmand, H. *et al.* Graphene nanoplatelets–silver hybrid nanofluids for enhanced heat transfer. *Energy conversion and management* **100**, 419–428 (2015).
26. Yarmand, H. *et al.* Study of synthesis, stability and thermo-physical properties of graphene nanoplatelet/platinum hybrid nanofluid. *International Communications in Heat and Mass Transfer* **77**, 15–21 (2016).
27. Yarmand, H. *et al.* Convective heat transfer enhancement with graphene nanoplatelet/platinum hybrid nanofluid. *International Communications in Heat and Mass Transfer* **88**, 120–125 (2017).
28. Abbasi, S. M., Rashidi, A., Nemati, A. & Arzani, K. The effect of functionalisation method on the stability and the thermal conductivity of nanofluid hybrids of carbon nanotubes/gamma alumina. *Ceramics International* **39**(4), 3885–3891 (2013).
29. Sajid, M. U. & Ali, H. M. Thermal conductivity of hybrid nanofluids: a critical review. *International Journal of Heat and Mass Transfer* **126**, 211–234 (2018).
30. Van Trinh, P. *et al.* Experimental study on the thermal conductivity of ethylene glycol-based nanofluid containing Gr-CNT hybrid material. *Journal of Molecular Liquids* **269**, 344–353 (2018).
31. Sumathi, S., Rajesh, R. & Subburaj, P. Investigation of Dielectric Strength of Transformer Oil Based on Hybrid TiO₂/Al₂O₃/MoS₂ Nanofluid Using Taguchi and Response Surface Methodology. *IETE Journal of Research*, 1–9 (2019).
32. Gupta, M. *et al.* Up to date review on the synthesis and thermophysical properties of hybrid nanofluids. *Journal of cleaner production* **190**, 169–192 (2018).
33. Kumar, D. D. & Arasu, A. V. A comprehensive review of preparation, characterization, properties and stability of hybrid nanofluids. *Renewable and Sustainable Energy Reviews* **81**, 1669–1689 (2018).
34. Andersson, H. I. & Valnes, O. A. Flow of a heated ferrofluid over a stretching sheet in the presence of a magnetic dipole. *ActaMechanica* **128**(1–2), 39–47 (1998).
35. Zeeshan, A., Majeed, A. & Ellahi, R. Effect of magnetic dipole on viscous ferrofluid past a stretching surface with thermal radiation. *Journal of Molecular liquids* **215**, 549–554 (2016).
36. Muhammad, N. & Nadeem, S. Ferrite nanoparticles Ni-ZnFe₂O₄, Mn-ZnFe₂O₄ and Fe₂O₄ in the flow of ferromagnetic nanofluid. *The European Physical Journal Plus* **132**(9), 377 (2017).
37. Rashidi, M. M., Ganesh, N. V., Hakeem, A. A., Ganga, B. & Lorenzini, G. Influences of an effective Prandtl number model on nano boundary layer flow of γ -Al₂O₃-H₂O and γ -Al₂O₃-C₂H₆O₂ over a vertical stretching sheet. *International Journal of Heat and Mass Transfer* **98**, 616–623 (2016).
38. Hayat, T., Shah, F., Khan, M. I., Khan, M. I. & Alsaedi, A. Entropy analysis for comparative study of effective Prandtl number and without effective Prandtl number via γ -Al₂O₃-H₂O and γ -Al₂O₃-C₂H₆O₂ nanoparticles. *Journal of Molecular Liquids* **266**, 814–823 (2018).
39. Lee, S., Choi, S. S., Li, S. A. & Eastman, J. A. Measuring thermal conductivity of fluids containing oxide nanoparticles. (1999).
40. Wang, X., Xu, X. & Choi, S. U. Thermal conductivity of nanoparticle-fluid mixture. *Journal of thermophysics and heat transfer* **13**(4), 474–480 (1999).

Acknowledgements

The authors acknowledge the financial support provided by the Center of Excellence in Theoretical and Computational Science (TaCS-CoE), KMUTT.

Author contributions

T.G. and A.K. modeled and solved the problem. M.B. and S.M. wrote the manuscript. T.G. and P.K. made the corrections. P.K., N.A.A. and Z.S. contributed in the numerical finding and English editing. All the authors have approved the manuscript.

Competing interests

The authors declare no competing interests.

Additional information

Correspondence and requests for materials should be addressed to P.K.

Reprints and permissions information is available at www.nature.com/reprints.

Publisher's note Springer Nature remains neutral with regard to jurisdictional claims in published maps and institutional affiliations.



Open Access This article is licensed under a Creative Commons Attribution 4.0 International License, which permits use, sharing, adaptation, distribution and reproduction in any medium or format, as long as you give appropriate credit to the original author(s) and the source, provide a link to the Creative Commons license, and indicate if changes were made. The images or other third party material in this article are included in the article's Creative Commons license, unless indicated otherwise in a credit line to the material. If material is not included in the article's Creative Commons license and your intended use is not permitted by statutory regulation or exceeds the permitted use, you will need to obtain permission directly from the copyright holder. To view a copy of this license, visit <http://creativecommons.org/licenses/by/4.0/>.

© The Author(s) 2020